Proceedings 10th NUMGE 2023
10th European Conference on Numerical Methods in Geotechnical Engineering
Zdravkovic L, Kontoe S, Taborda DMG, Tsiampousi A (eds)

https://doi.org/10.53243/NUMGE2023-381

Influence of pipe arrangement and improved thermal conductivity on the response of thermo-active piles

D.M.G. Taborda[1], M.S. Bortolotto[1], R.Y.W. Liu[1]

[1]*Department of Civil and Environmental Engineering, Imperial College London, London, UK*

ABSTRACT: This paper investigates the mechanical effects of introducing an additional zone of improved thermal conductivity surrounding a thermo-active pile and its interaction with the adopted pipe arrangement. A simplified method, that avoids the explicit modelling of heat exchanger pipes in three-dimensional analysis, is adopted to reduce the computational cost of the performed parametric study. According to this method, a two-dimensional transient thermal analysis of the cross-section of the pile is first used to establish the average temperature along the circle containing the heat exchanger pipes. This average temperature is then employed as the thermal load in an axisymmetric thermo-hydro-mechanical analysis of the pile, from where axial stresses can be obtained. The results suggest that improving the thermal conductivity of a small zone of soil around the pile leads to a reduction in the calculated peak thermally-induced axial stress. Greater reductions are generally associated with larger zones and larger improvements in thermal conductivity. Conversely, the increase in the number of heat exchanger pipes is shown to lead to higher temperatures being achieved sooner and, therefore, to higher thermally-induced axial stresses.

Keywords: energy geotechnics; thermo-active structures; thermo-hydro-mechanical interaction; foundations; design

1 INTRODUCTION

Ground Source Energy Systems (GSES) are expected to play a major role in decarbonising heating and cooling systems and are attractive for large buildings and infrastructure as they can be deployed by equipping the foundations and retaining walls with heat exchanger pipes. This reduces capital costs as it avoids additional drilling since these geotechnical structures are already required for stability. A review of the design and behaviour of these structures is available in Loveridge et al. (2020), where the importance of ground conditions, particularly in terms of thermal properties, is emphasised. Clearly, larger thermal conductivity of the ground is associated with better thermal performances or, equivalently, lower costs of GSESs. Therefore, there would be a clear benefit arising from a possible ground improvement technique focusing on the role of the ground as a thermal energy storage medium. This paper explores the thermo-mechanical interactions associated with thermo-active piles embedded in a zone of soil with improved thermal properties, investigating the effects of the thickness and thermal conductivity of this zone, and the importance of different heat exchanger pipe arrangements in this context.

2 NUMERICAL ANALYSIS

2.1 Methodology and description of the problem

The development of structural forces within a single 900 mm diameter thermo-active pile installed in London Clay and subjected to continuous heating for 180 days is considered in this study. Two main factors are being investigated in the analyses presented herein: (i) the effect of improving the thermal conductivity, λ, in a limited zone around the thermo-active pile extending radially to $r = r_i > R$ (where R is the radius of the pile, see Figure 1(a)), and (ii) the impact of different pipe arrangements. Clearly, the complete modelling of this problem would require a three-dimensional (3D) coupled thermo-hydro-mechanical (THM) analysis involving the explicit simulation of heat exchanger pipes. However, such analyses are computationally expensive and require numerical algorithms that are seldom available, such as upwinding schemes or the Petrov-Galerkin method (Gawecka et al., 2020). Therefore, the simplified method proposed by Liu et al. (2020) is adopted as it replaces the aforementioned 3D coupled THM analyses by a combination of a thermal analysis of the cross-section of the pile (Figure 1(a)) and a coupled THM axisymmetric analysis of the thermo-active pile (Figure 1(b)). Clearly, these analyses are substantially simpler and more computationally efficient, with Liu et al. (2020) showing that the proposed approach reproduces the thermal fields and the resulting structural forces within the thermo-active piles with excellent accuracy.

The first analysis prescribed by the method presented in Liu et al. (2020) is a simple thermal analysis of the cross-section of the pile (i.e. performed in plan view), with the location of the different pipes modelled accurately. In general, these are equally spaced around the pile at a radial distance from its axis of $r = r_p$, though

this is not strictly required by the method. At each of these locations, the estimated fluid temperature is applied to the pipes as a boundary condition to the problem. While in the present case this will be a constant temperature, this method is expected to remain accurate for transient fluid temperatures, such as those arising from realistic heat pump operational patterns. Liu et al. (2020) suggest that, for a given u-loop where the inlet temperature T_{in} is assumed to be constant, the temperature boundary conditions to be applied at the position of the pipes should approximate those expected at mid-depth of the pile ($T_{in,mid}$, $T_{out,mid}$). Given an estimated thermal performance of the pile of ΔE [kW/m], this leads to:

$$T_{in,mid} = T_{in} - \frac{1}{4} \cdot \frac{\Delta E \cdot L_{pile}}{n_{loops} \cdot (\rho c)_f \cdot Q_f} \quad (1)$$

$$T_{out,mid} = T_{in} - \frac{3}{4} \cdot \frac{\Delta E \cdot L_{pile}}{n_{loops} \cdot (\rho c)_f \cdot Q_f} \quad (2)$$

where L_{pile} is the length of the pile [m], n_{loops} is the number of u-loops within the pile, $(\rho c)_f$ is the volumetric heat capacity of the fluid [kJ/(m^{3}K)] and Q_f is the flow rate per u-loop [m^3/s].

Following the thermal analysis, for each time instant t_i, the distribution of temperatures along the circle that contains the axes of the various heat exchanger pipes, $T(\theta, t_i)$ (the dashed line in Figure 1(a)), is determined. Subsequently, the average of each temperature distribution $T_{BC}(t_i)$ is computed using the mean value theorem for integrals:

$$T_{BC}(t_i) = \frac{1}{2\pi} \int_0^{2\pi} T(\theta, t_i) d\theta \quad (3)$$

which, for the simple case of equispaced points along the circle, reduces to the average temperature.

The generated temperature time series is then applied as a boundary condition along a vertical line positioned at $r = r_p$ in an axisymmetric analysis (Figure 1(b)). Unlike in the previously described thermal analysis, where only the thermal behaviour of the materials was modelled, this second analysis takes into account the fully coupled THM response of the soil and improved area. The average axial stress in the pile ($\overline{\sigma_{axial}}(z, t_i)$) can then be computed by integrating the axial stresses ($\sigma_{axial}(z, r, t_i)$) within its section at each depth z:

$$\overline{\sigma_{axial}}(z, t_i) = \frac{1}{\pi R^2} \int_0^R 2\pi r \cdot \sigma_{axial}(z, r, t_i) dr \quad (4)$$

where R is the radius of the pile being modelled.

Clearly, while simple, the procedure outlined above requires the extraction and processing of substantial amounts of data. In the present study, all these operations were automated by using the *Python* API available in PLAXIS2D (Bentley Systems, 2022).

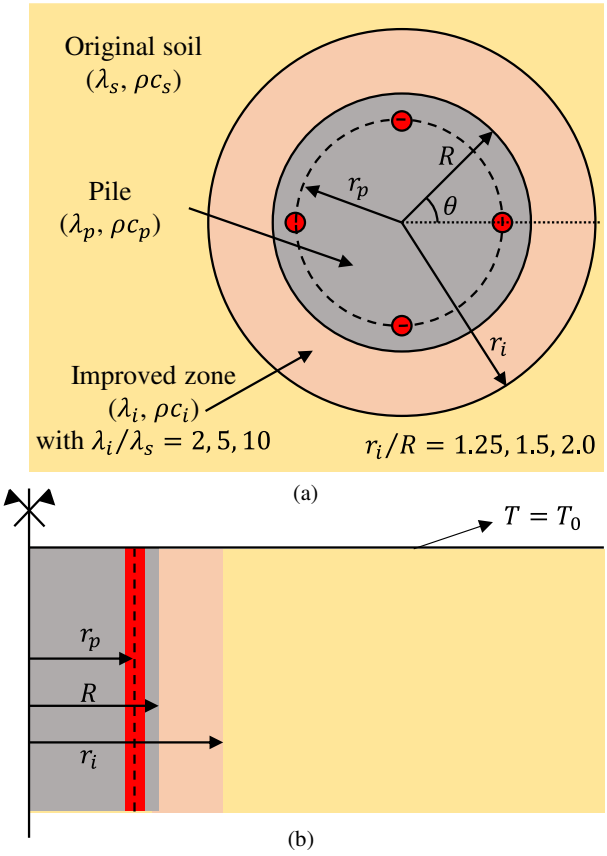

Figure 1. Geometric description of the problem in terms of (a) plan view and (b) side view.

Table 1. Applied boundary conditions in terms of changes in temperature for three pipe arrangements.

Number of loops n_{loops}	$T_{in,mid}$ (Equation 1)	$T_{out,mid}$ (Equation 2)
1	38.1 °C	35.2 °C
2	38.8 °C	37.3 °C
3	39.0 °C	38.1 °C

2.2 Thermal analysis

The first step of the Liu et al. (2020) method requires a transient thermal 2D analysis of the cross-section of the thermo-active pile. Three distinct pipe arrangements are considered in this study, as listed in Table 1 together with the values of $T_{in,mid}$ (Equation 1) and $T_{out,mid}$ (Equation 2), obtained for a pile with a length L_{pile} of 25 m assuming a thermal performance of ΔE = 99 W/m (based on values recommended by Brandl (2006), see Liu et al. (2020)), a volumetric heat capacity of the fluid $(\rho c)_f$ = 4190 kJ/(m^{3}K), a flow rate per u-loop of Q_f = 1.03E-04 m^3/s and a fixed inlet temperature of T_{in} = 39.5 °C (i.e. 20 °C above natural ground temperature, see Liu et al. (2020)). The pipes were assumed to have an inner diameter of 26.4 mm and a concrete cover of 70 mm. As expected, when the number of u-loops increases, it leads to a reduction in the heat losses associated with each u-loop and, consequently, to an increase in the estimated operating temperatures.

For the required type of analysis, only the thermal properties of the various materials need to be specified (i.e. λ and (ρc)). These are listed in Table 2 and are based on the properties used by Gawecka et al. (2017) and Liu et al. (2020). For the improved soil, different multiples of the thermal conductivity of London Clay were used, i.e. λ_i = k λ_s, with k = 2, 5 and 10, with the last value representing an upper limit to the influence of the improved zone on the behaviour of the pile. Four distinct cases were considered for the size of the improved zone: the reference case (i.e. no improvement), and r_i/R = 1.25, 1.50 or 2.00. Figure 2 shows the results of three analyses selected among those performed in terms of temperature along the circle with radius $r = r_p$ (the dashed line in Figure 1(a)). To illustrate the magnitude of the obtained circumferential variations in temperature, a relatively short period of operation was chosen (5 days). In one of these analyses (red line), the radius of the improved zone was set to be twice that of the pile (i.e. forming an annulus with a thickness equal to that of the pile radius), while its thermal conductivity was 5 times larger than that of the original soil. Clearly, by improving the thermal conductivity in a small area around the pile and thus the heat transfer between pile and surrounding ground, the calculated temperatures drop by about 1 °C in the zones away from the heat exchanger pipes. Conversely, by increasing the number of u-loops from 1 (blue line) to 3 (black line), the overall temperatures increase substantially, due to the greater density of heat sources.

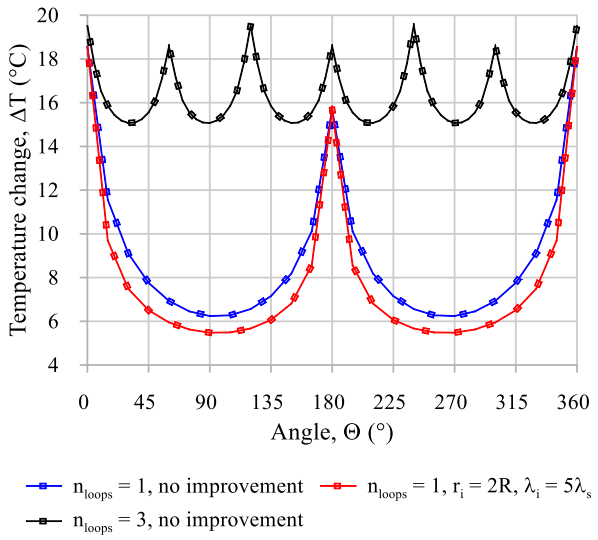

Figure 2. Changes in temperature (i.e. above initial ground temperature) along the circle of radius r_p after 5 days of heating for three selected cases.

Table 2. Material properties used in the thermal analyses.

Material	Thermal conductivity λ [W/mK]	Volumetric heat capacity (ρc) [kJ/(m^{3}K)]
Concrete	2.33	1920.0
London Clay	1.79	1820.0

2.3 *Thermo-hydro-mechanical analysis*

The second step of the Liu et al. (2020) method requires the calculation of a time series representing the average temperature at the circle containing the heat exchanger pipes as computed in the thermal analyses described in the previous section. In the present case, this process was largely automated using the *Python* API available in PLAXIS2D, resulting in the data shown in Figure 3, which covers the entire 180 days of heating applied to the pile. For the previously considered cases, the obtained evolutions of average temperatures confirm further that the increase in the number of u-loops leads to larger temperatures, with a difference of about 6 °C between the 1 u-loop case (blue line) and the 3 u-loop case (black line). Interestingly, the effect of introducing an area of improved thermal conductivity (in this case, r_i/R = 2, λ_i/λ_s = 5, red line) seems to be limited to the first 30-60 days (a drop of about 1 °C in average temperature). In effect, any gains in thermal performance eventually vanish, as the results show that at 180 days there is no practical influence of the improved area.

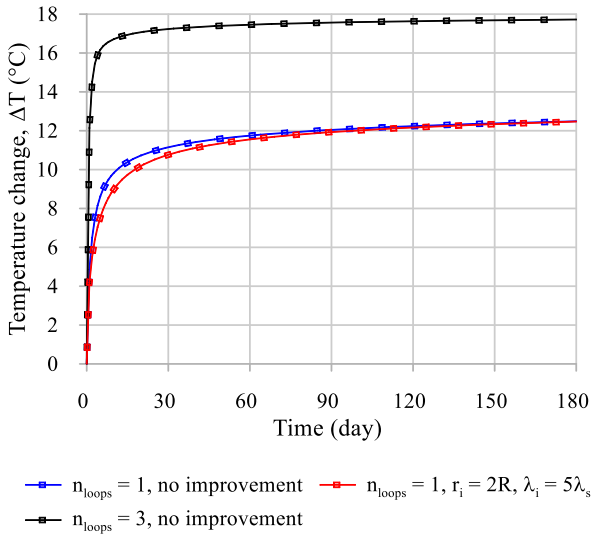

Figure 3. Variations with time of the average temperature change for three selected cases.

Temperature time histories such as those shown in Figure 3 are subsequently introduced as the boundary condition along the vertical line denoting the position of the heat exchanger pipes, as shown in Figure 1(b). Clearly, these coupled analyses require the definition of additional parameters to those listed in Table 2, such as those governing the material's hydro-mechanical behaviour. The concrete pile is assumed to be linear-elastic, characterised by a Young's modulus E = 30 GPa and a Poisson's ratio ν = 0.3. Conversely, the behaviour of the London Clay is described using a non-linear elastic, perfectly-plastic model. Its strength is assumed to be defined by a non-associated Mohr-Coulomb failure criterion, while its stiffness is simulated using the small strain

stiffness model IC.G3S proposed by Taborda et al. (2016):

$$G_{tan} = G_{ref} \cdot \left(\frac{p'}{p'_{ref}}\right) \cdot \left(R_G + \frac{1-R_G}{1+\left(\frac{E_d}{a}\right)^b}\right) \quad (5)$$

$$K_{tan} = K_{ref} \cdot \left(\frac{p'}{p'_{ref}}\right) \cdot \left(R_K + \frac{1-R_K}{1+\left(\frac{|\varepsilon_{vol}|}{r}\right)^s}\right) \quad (6)$$

where p' [kPa] is the mean effective stress, p'_{ref} = 101.3 kPa is a reference pressure, E_d [m/m] is the generalised deviatoric strain (i.e. the second invariant of the strain tensor) and ε_{vol} [m^3/m^3] is the volumetric strain (i.e. the first invariant of the strain tensor), G_{ref} [kPa] and K_{ref} [kPa] are a reference shear modulus and bulk modulus, respectively, a, b and R_G are dimensionless stiffness reduction parameters for calculating the tangent shear modulus, G_{tan} [kPa], while r, s and R_K are the corresponding dimensionless parameters for the tangent bulk modulus, K_{tan} [kPa]. This material model was implemented as a User-Defined Soil Model (UDSM) in PLAXIS2D, as described in Taborda et al. (2023). Lastly, the improved material around the pile, when present, is assumed to behave like the original London Clay, with the only difference being its thermal conductivity. The full set of parameters is presented in Table 3.

Table 3. Adopted hydro-mechanical parameters used in the analysis.

Material	Parameters
Concrete pile	*Mechanical behaviour* Linear-elastic E = 30 GPa, $\nu = 0.3$ *Hydraulic behaviour* Non-porous
London Clay	*Mechanical behaviour* Non-linear elastic, perfectly-plastic ϕ' = 25°, ψ = 12.5°, c' = 5 kPa G_{ref} = 51.7 MPa, a = 5.60E-5, b = 0.90, R_G = 0.06450, K_{ref} = 26.7 MPa, r = 1.27E-4, s = 1.80, R_K = 0.13275 *Hydraulic behaviour* k = 1E-10 m/s

In the axisymmetric THM analyses, the initial stress conditions are generated using a saturated bulk unit weight for London Clay of 20 kN/m^3 and an at-rest coefficient of earth pressure of K_0 = 1.0 (constant with depth). The water table is assumed to be positioned at the ground surface, with a hydrostatic pore water pressure profile being adopted. Moreover, given that the pile is 25m long and has a radius of 450 mm, the mesh dimensions are set to 64m high and 45 m wide (i.e. 100 times larger than the pile radius). The horizontal displacement of the nodes pertaining to the lateral boundaries are restricted, while the nodes within the bottom boundary are restricted along both directions (vertical and radial). The final mechanical boundary condition relates to an initial compressive axial load, applied as a uniform stress at the nodes defining the top of the pile. The same sequence as that described in Liu et al. (2020) is followed, with a load of 2900 kN (4560 kPa) being applied, corresponding to an estimated factor of safety in terms of axial capacity of about 2.6. Subsequently, a sufficiently large period of time is modelled in order to allow the complete dissipation of excess pore water pressures, thus separating the effect of thermal loading from any transient phenomena associated with consolidation processes taking place as a result of mechanical modelling. The hydraulic boundary conditions used in these analyses include a *seepage* condition at the surface (i.e. water is allowed to flow towards the outside of the mesh, but not towards the inside), while all the remaining boundaries (the axis of symmetry, the base of the mesh and the far-field) are set to *impervious*. The thermal load is applied for 180 days as a specified temperature along a vertical line positioned at $r = r_p$ (see Figure 1(b)), with values given by the 2D thermal analyses (e.g. Figure 3). The ground surface is assumed to remain at a constant temperature, equal to the initial temperature of the soil (19.5 °C), while the axis of symmetry, bottom boundary of the mesh and far-field are all set to adiabatic (i.e. no heat flux). The results of these analyses are described in detail in the subsequent section.

3 RESULTS

3.1 Improved thermal conductivity

In the first set of analyses, the effects of the zone of soil with an improved thermal conductivity on the behaviour of a pile equipped with two u-loops is studied. In addition to the reference case, where only the original soil deposit is considered (i.e. 'no improvement'), nine analyses corresponding to different combinations of extent of improved zone (r_i/R = 1.25, 1.5 and 2.0) and improved thermal conductivity (λ_i/λ_s = 2, 5 and 10) are performed. The results are summarised in Figure 4, in terms of peak thermally-induced axial stress (Figure 4(a)) and in terms of variation of this quantity with respect to the 'no improvement' case (Figure 4(b)).

In general, compressive forces are induced by pile heating as the soil restricts the thermal expansion of the pile. This leads to an increase in axial force. However, as the heat propagates to the surrounding soil, leading to its thermal expansion and, therefore, to a reduction in the 'differential' expansion between the pile and the soil, the

thermally-induced axial forces are expected to drop over time after reaching a peak. This transient behaviour, described in detail in Gawecka et al. (2017) and Liu et al. (2020), means that the peak thermally-induced axial stresses shown in Figure 4 are necessarily observed in the short term (after about 3-6 days of heating). Given the above, the behaviour obtained in the performed analyses is perhaps unsurprising: adding a zone of higher thermal conductivity promotes radial heat flux, reducing the temperatures in the pile and increasing those of the soil, with both effects resulting in a decrease of the 'differential' thermal expansion responsible for the increase in pile axial stress. Reductions of up to 12%, 26% and 32% are obtained for a thickness of the improved zone equal to the pile radius ($r_i/R = 2$) and thermal conductivity improvement ratios of 2, 5 and 10, respectively. It is also interesting to note that, particularly for the lowest value of $\lambda_i/\lambda_s = 2$, the reduction in axial stress is considerably non-linear, with the thickness of the improved zone having a smaller impact above a certain value.

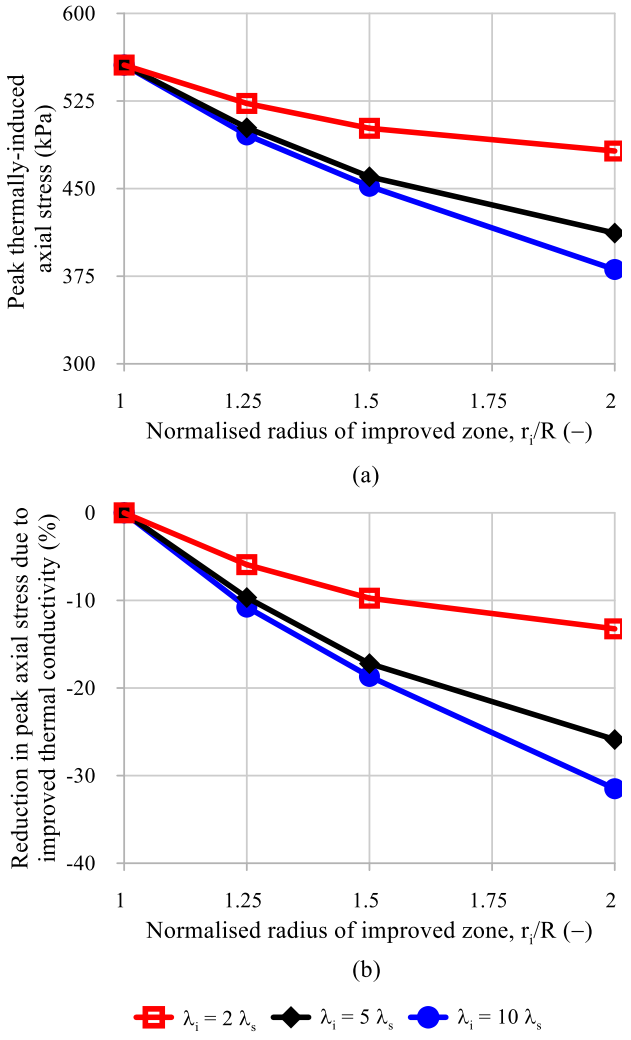

Figure 4. Effect of radius of improved zone and improved thermal conductivity for a pile with 2 u-loops: (a) changes in peak thermally-induced axial stress and (b) relative variation in stress compared to the case without any improvement.

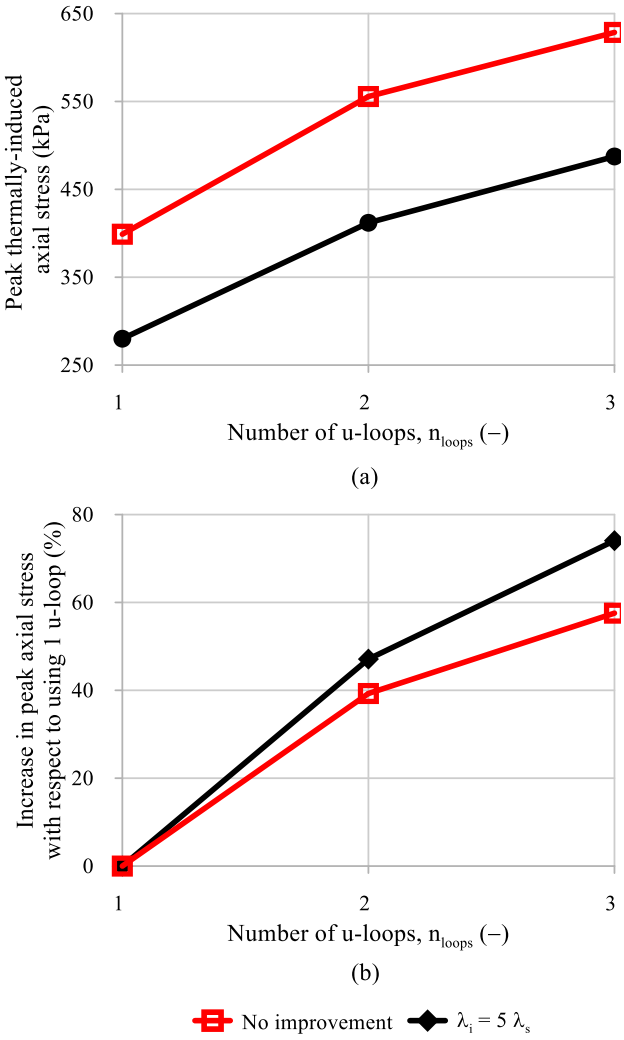

Figure 5. Effect of number of u-loops and presence of improved zone with $r_i/R = 2$: (a) changes in peak thermally-induced axial stress and (b) relative variation in stress compared to the 1 u-loop case.

3.2 Pipe arrangement

A similar set of analyses are performed to investigate the impact of changing the pipe arrangement and its interaction with the zone of improved thermal conductivity: the number of u-loops is varied from 1 to 3, for both the reference case ('no improvement') and a case where the thickness of the improved zone with $\lambda_i/\lambda_s = 5$ is equal to the pile radius (i.e. $r_i/R = 2$). The obtained results are shown in Figure 5 where it can be seen that the adoption of a larger number of loops leads to a substantial increase in the axial stress sustained by the pile. For the 'no improvement' analyses, in comparison with the 1 u-loop case, the use of 2 u-loops results in a 40% increase in axial stress, while the use of 3 u-loops leads to a 60% increase in axial stress. This is the same trend as that observed in Liu et al. (2020) for a pile subjected to similar thermal loading modelled in 3D with the explicit inclusion of heat exchanger pipes, further confirming the high accuracy of the proposed simplified method. As discussed in the previous section, the introduction of a zone with improved thermal conductivity generally reduces

the thermally-induced axial stresses. This can be observed in Figure 5(a), where the increase in axial stresses are, on average, about 100 kPa lower for each of the three pipe arrangements used when $\lambda_i/\lambda_s = 5$. This means that, when normalised with respect to the 1 u-loop case, the introduction of additional u-loops results in steeper increases in axial stress when a zone of improved thermal conductivity exists. In effect, as shown in Figure 5(b), the use of 2 u-loops leads to a 50% increase in axial stress, while 3 u-loops results in an increase of almost 80% (for $\lambda_i/\lambda_s = 5$).

Clearly, the use of a larger number of u-loops counteracts the effect of introducing a zone of improved thermal conductivity, since the former leads to a reduction in temperature through enhanced radial heat flux, while the latter results in an increase in pile temperatures due to the larger number of heat sources within the cross-section of the pile. However, the two factors have different impacts on the time taken to reach the peak axial stress, with the number of u-loops leading to faster heating of the piles, thus reducing the time corresponding to the peak thermally-induced axial stress from about 5 days (1 u-loop) to 2.5 days (3 u-loops). These values match the trends shown by Liu et al. (2020) using 3D analyses and, in the present study, are observed to be generally independent of the presence of a zone with improved thermal conductivity and of its characteristics (thickness and improvement ratio).

4 CONCLUSIONS

This paper demonstrates the application of the simplified method proposed by Liu et al. (2020) to the investigation of the effects of adding a zone of improved thermal conductivity around a thermo-active pile installed in London Clay and its interaction with the adopted pipe arrangement. While these two aspects of the pile-soil system are likely to have a substantial effect on its thermal performance, the present study focuses primarily on its thermo-mechanical response. In addition to the reference case (i.e. 'no improvement'), the considered analyses include three different thicknesses of improved zone (25%, 50% and 100% of the pile radius), three improvement ratios (thermal conductivity increased to 2, 5 and 10 times its original value within the improved zone) and three pipe arrangements (1, 2 and 3 u-loops). These analyses were defined parametrically, allowing the development of a script that sets up, calculates and post-processes the analyses in an automated way using PLAXIS2D's Python API, thus streamlining the workflow for exploring the response of thermo-active piles.

The results show that introducing a zone of improved thermal conductivity has a beneficial effect, reducing the peak thermally-induced mechanical stress to which the pile is subjected. This is attributed to the associated enhanced radial heat flux, which reduces the maximum temperatures within the pile, while increasing those of the soil. These two factors contribute to a reduction of the 'differential' thermal expansion of the pile-soil system, which is the main driver for thermally-induced axial stresses. While a larger improved zone leads to a greater reduction in peak axial stress, the incremental effect reduces with the thickness of the improved zone, suggesting that beyond a certain threshold there is little to be gained from improving the thermal properties of the soil surrounding the pile. This is particularly evident for low values of improvement ratio λ_i/λ_s.

In terms of pipe arrangement, the observed effects match those reported in Liu et al. (2020) and are shown to be independent of the presence of the zone of improved soil. The adoption of a larger number of u-loops increases the density of heat sources (i.e. number of pipes per m of perimeter of pile), leading to overall faster increases and larger average temperatures within the pile, translating into higher thermally-induced axial stresses which are observed sooner in the heating process.

5 ACKNOWLEDGEMENTS

This research is part of the SaFEGround (Sustainable, Flexible and Efficient Ground-source heating and cooling systems) project, which is funded by the Engineering and Physical Sciences Research Council (EPSRC) (grant number: EP/V042149/1).

6 REFERENCES

Bentley Systems (2022) *CONNECT Edition V22 PLAXIS 2D Reference Manual*.

Brandl, H. 2006. Energy foundations and other thermo-active ground structures. *Geotechnique* **56(2)**, 81-122.

Gawecka, K.A., Taborda, D.M.G., Potts, D.M., Sailer, E., Cui, W., Zdravković, L. 2020. Finite-element modeling of heat transfer in ground source energy systems with heat exchanger pipes. *International Journal of Geomechanics*, **20(5)**, 04020041.

Gawecka, K.A., Taborda, D.M.G., Potts, D.M., Cui, W., Zdravković, L., Haji Kasri, M.S. 2017. Numerical modelling of thermo-active piles in London Clay. *ICE Proceedings: Geotechnical Engineering* **170(3)**, 201-219.

Liu, R.Y.W., Sailer, E., Taborda, D.M.G., Potts, D.M., Zdravković, L. 2020. A practical method for calculating thermally-induced stresses in pile foundations used as heat exchangers. *Computers and Geotechnics* **126**, 103743.

Loveridge, F., McCartney, J.S., Narsilio, G.A., Sanchez, M. 2020. Energy geostructures: a review of analysis approaches, in situ testing and model scale experiments. *Geomechanics for Energy and the Environment* **22**, 100173.

Taborda, D.M.G., Kontoe, S., Tsiampousi, A. 2023. IC MAGE Model 01 - strain-hardening/softening Mohr-Coulomb failure criterion with isotropic small strain stiffness (version 2.0). *Zenodo*. doi: 10.5281/zenodo.7565062

Taborda, D.M.G., Potts, D.M., Zdravkovic, L. 2016. On the assessment of energy dissipated through hysteresis in finite element analysis, *Computers and Geotechnics* **71**,180-194.